



An exploration on retro-construction of plasma drug concentration-time curves from corresponding urine excretion data and single-point plasma concentrations using a simplified and idealized method

Guanglu Li^{1#}, Wenpeng Zhang^{1#}, Meng Zhang^{2#}, Jiamin Xu², Guanghua Zhu², Jinglai Li³, Huan Luo³, Xiaomei Zhuang¹, Qunjun Wang¹, Tianhong Zhang^{1,3}

¹State Key Laboratory of Toxicology and Medical Countermeasures, Beijing Institute of Pharmacology and Toxicology, Beijing, China; ²Department of Clinical Research Center, Beijing Children's Hospital, Capital Medical University, National Center for Children's Health, Beijing, China; ³Guoke Excellence (Beijing) Medicine Technology Research Co., Ltd., Beijing, China

Contributions: (I) Conception and design: Q Wang, T Zhang; (II) Administrative support: W Zhang, X Zhuang; (III) Provision of study materials or patients: M Zhang, J Xu, G Zhu, J Li, H Luo; (IV) Collection and assembly of data: G Li, W Zhang, M Zhang; (V) Data analysis and interpretation: G Li, W Zhang, M Zhang; (VI) Manuscript writing: All authors; (VII) Final approval of manuscript: All authors.

[#]These authors contributed equally to this work.

Correspondence to: Dr. Tianhong Zhang. Guoke Excellence (Beijing) Medicine Technology Research Co., Ltd., No. 18 Zhonghe Street, Daxing District, Beijing 10176, China. Email: wdzth@sina.com; Dr. Qunjun Wang. State Key Laboratory of Toxicology and Medical Countermeasures, Beijing Institute of Pharmacology and Toxicology, 27 Taiping Road, Haidian District, Beijing 100039, China. Email: wangqunjunbeijing@163.com.

Background: Despite the availability of various tools of modeling and simulation, clinical pediatric pharmacokinetic (PK) studies remain far less efficient than those on adults due to ethical constraints. One of the optimal solutions is to substitute urine to blood sampling based on explicit mathematic relationships between them. However, this idea is limited by three main knowledge gaps associated with urine data, i.e., complicated excretion equations with excessive parameters, insufficient frequency that is hard to fit, and the mere expression of amounts with no *in vivo* distribution volume information involved.

Methods: To overcome these obstacles, we sacrificed the precision from mechanistic PK models with complex excretion equations to expediency of compartmental model in which a constant k_e is used to cover all the internal parameters. And the total cumulative amounts of urinary drug excretion (X_u^∞) were estimated and introduced to the excretion equation so that urine data were likely to be fitted using a semi-log-terminal linear regression method. In addition, urinary excretion clearance (CL_r) could be calculated by single point plasma data to anchor the plasma concentration-time (C-t) curve based on the assumption that CL_r was kept constant throughout the PK process.

Results: After sensitivity analysis of two subjective judgements (the selection of the compartmental model and the selection of plasma time point to calculate CL_r), the performance of the optimized models was assessed using desloratadine or busulfan as model drugs in a variety of PK scenarios, from *i.v.* bolus/infusion to *p.o.* administration, from a single dose to multiple doses, and from rats to children. The fitting plasma drug concentrations of the optimal model were close to the observed value. Meanwhile, the drawbacks inherent to the simplified and idealized modeling strategy were fully identified.

Conclusions: The method proposed by this tentative proof-of-principle study was able to deliver acceptable plasma exposure curves and shed light on the future refinements.

Keywords: Pediatric; pharmacokinetics; modeling

Submitted Oct 09, 2022. Accepted for publication Mar 15, 2023. Published online Apr 20, 2023.

doi: 10.21037/tp-22-505

View this article at: <https://dx.doi.org/10.21037/tp-22-505>

Introduction

In recent years, health and drug regulators around the world have introduced a number of incentives and regulations for the industry in order to ensure children's access to innovative, safe, and effective medications (1). Accordingly, related basic research has become increasingly active and fruitful, resulting in better understanding of the difference between children and adults in drug absorption, distribution, metabolism, and excretion (ADME) characteristics caused by age/maturation-related enzyme/transporter expression and other physiological/pathological specifications (2,3). All the new knowledge can boil down to the best-known saying that children are not small adults (4).

Despite the amazing progress in basic research, few of the findings have been translated into clinical dosing recommendations due to inadequate clinical validation (5). Consequently, pediatric patients have not fully benefited from the achievements of pharmacological research. For instance, pediatric medications and drug development still lag far behind demand, such as pediatric exclusive medicines or extended applications in young populations from adult drugs. In addition, without adequate clinical data, "off-label" use and intuitive doses frequently occur in pediatric clinic, which is likely to trigger potential drug-induced toxicity, drug-drug interactions or treatment failure (6,7). It seems that children still remain "therapeutic orphans" proposed initially by Dr. Shirkey in 1962 (8,9).

Obviously, the main obstacle to this area is the lack of clinical pharmacokinetic (PK) data due to the limited number of children with a particular disease and the

difficulty in finding subjects restricted by ethical concerns. Another core problem is the fact that a full-sampling sophisticated clinical PK trial is undoubtedly infeasible in such fragile populations. Therefore, the quality of pediatric data with absence of individual PK profiles is extremely poor.

To overcome the drawbacks mentioned above, a variety of advanced technologies and novel research strategies have been applied to increase the accessibility and acceptability of the pediatric clinical PK data. For example, to facilitate the sampling process, strategies like micro-volume sampling, sparse sampling, opportunistic sampling, and surrogate sampling (such as saliva, exhaled gas) have been used in pediatric clinical trial protocols (10,11). Alongside that, a series of mathematical modeling methods has been used in data mining to maximize findings from limited data. There are two main strategies in modeling and simulation (M&S). One is the top-down modeling strategy, represented by population PK (popPK) analysis, which integrates sparse data to characterize the PK of pediatric populations or extrapolates the pediatric PK from adults' data by means of statistics (12). The other one is the bottom-up modeling strategy, represented by physiologically based pharmacokinetic (PBPK) modeling, which combines the physiochemical property of the compound and the physiological parameters of the population to predict the PK properties using mechanism-based mathematic tools (13). Both M&S tools help to replace or reduce pediatric clinical data requirements to some extent (10), but neither can fully address the challenges of pediatric clinical studies, such as the lack of subjects, time-consuming experimentation, and the absence of individual full exposure curves. Frankly, the data quality has not been substantially improved.

So far, the public perception has been changed from "it is unethical to test drugs in children" to "it is unethical to give children medications without sufficient clinical verifications". In the meantime, the same evidentiary criteria for adults should be adopted for pediatric innovative drug approval (14). However, this is virtually impossible without high-quality individual exposure curves. Therefore, it is imperative to develop a novel approach that can quantitatively depict the individual full PK profiles within practical and ethical compliance.

Non-invasive sampling is considered the most promising method, where urine is an optimal surrogate matrix to analysis with significant advantages. In detail, urine collection is easy without any ethical concerns so that

Highlight box

Key findings

- A non-invasive sampling strategy in which urine is used as surrogate matrix in PK trial was introduced and validated in this study.

What is known and what is new?

- There are three main knowledge gaps about urinary data, which are the complicated excretion mechanism, insufficient frequency sampling, and the absent volume information.
- Using simplified and idealized tactics to cross the gaps, the present modeling approach was able to produce acceptable plasma exposure curves with some limitations which were fully discussed.

What is the implication, and what should change now?

- The proposed method might promote the good practice of clinical trials in pediatric populations by updating the research paradigm.

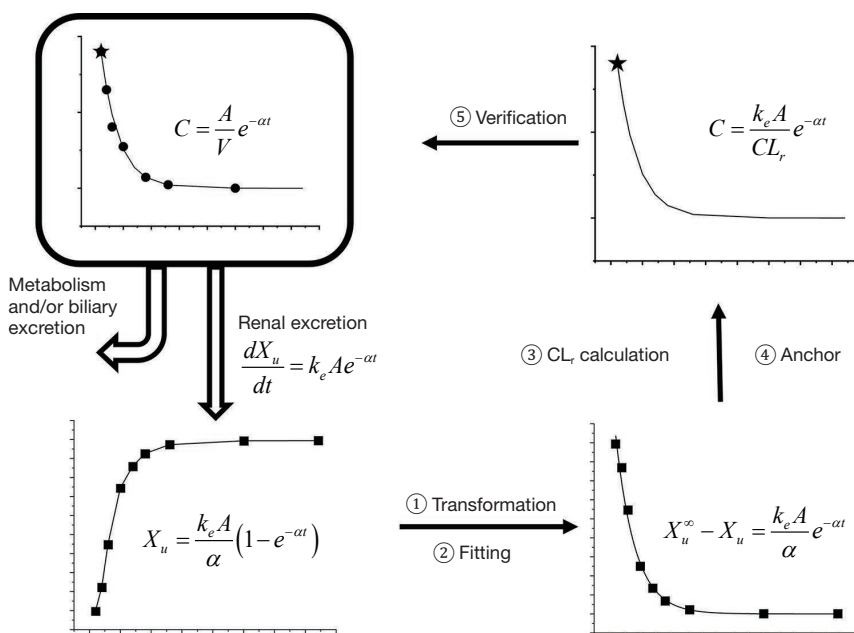


Figure 1 A schematic description of the proposed method to retro-construct a plasma drug concentration time curve by the urinary excretion data and a single-point plasma concentration, taking one-compartment model with *i.v.* bolus administration as example. ① The observed cumulative urinary excretion data was transformed into the residual urinary drug amount. ② The resulting $(X_u^\infty - X_u) - t$ was fitted to get the parameters α and $k_e A$, which ③ was further used to calculate CL_r , based on a single-point plasma concentration (*). Then ④ the C-t curve could be anchored by CL_r and ⑤ could be verified by comparing the predicted and the observed plasma concentrations at each time point. C-t, concentration-time; CL_r , urinary clearance.

the number of children enrolled in clinical trials will be increased by the reduced burden of blood sampling, and therefore the quality of PK data will be enhanced by the availability of full description of individual PK profiles.

The primary task of this vicarious method is the construction of a mathematical model that can bridge the drug exposure between urine and plasma. Several major knowledge gaps during modeling have to be overcome and the corresponding solutions we proposed are listed as follows. (I) Urinary drug excretion is a complex procedure (filtration, secretion, and reabsorption) with multiple factors that can hardly be quantified exhaustingly. Our workaround is using the urinary drug excretion rate constant (k_e) to cover all the parameters in urinary excretion no matter how complicated the mechanism is. In other words, the classical compartmental models characterized by simplicity, appearance, and approximation were used in our modeling instead of the contemporary commonly accepted PBPK models characterized by complexity, mechanism, and precision. (II) Even on a simple compartmental model, based on insufficiently frequent urine samples, the urinary

excretion equation is too complex to fit. To fix this problem, the total cumulative amounts of urinary drug excretion (X_u^∞) were estimated and the residual urinary amounts ($X_u^\infty - X_u$) were calculated, leading to a simplified equation that can be fitted. Take the simplest one-compartment model with *i.v.* bolus administration in *Figure 1*, the $X_u - t$ curve was transformed to $(X_u^\infty - X_u) - t$ curve in the first step for easier fitting. The fitted slope (exponential term, $-\alpha$) of $(X_u^\infty - X_u) - t$ curve was found to be of the same slope as concentration-time (C-t) curve. That means the slope of plasma C-t curve could be fitted by urinary data. (III) However, since there is no any volume information in urinary equations, to construct a plasma C-t curve equation, urinary clearance (CL_r) as an indispensable parameter was calculated using a single-point plasma concentration based on an assumption that CL_r was constant during the whole ADME procedure. Finally, the definite plasma C-t curve equation could be constructed approximately.

Practically, more complicated scenarios have occurred than the one-compartment model with *i.v.* bolus administration in *Figure 1*, such as multiple compartmental

models with *i.v.* infusion, *p.o.*, and/or multiple doses. To cover these scenarios, desloratadine and busulfan (the reported PK characters of them are summarized in Table S1), both are first-line drugs in pediatric for anti-allergy and anti-leukemia treatments, were selected as model drugs. In addition, there are two subjective judgments that need to be made in the modeling process: one is the selection of a compartmental model, and the other is the selection of a time-point plasma concentration to calculate CL_r . Both are optimized by sensitivity analysis, and the proximity of the final model to the observed value is assessed either in rats or in children. We present the following article in accordance with the ARRIVE reporting checklist (available at <https://tp.amegroups.com/article/view/10.21037/tp-22-505/rc>).

Methods

Rationale

The model was based on assumption that elimination pathways of the test drug *in vivo* should include renal excretion whose process is consistent with first order kinetic with a constant k_e . To specify the compartmental models and the dosing regimens, the model was preliminarily divided into 6 scenarios and listed below. The corresponding equations were quoted from reference (15) with minor rearrangement for more explicit illustration of the relationship in drug exposure between urine and plasma.

Scenario 1, one-compartment model after single dose *i.v.* bolus administration

The *in vivo* drug amount-time profile of the one-compartment distribution model after single dose *i.v.* administration follows Eq. [1.1]

$$X = Ae^{-\alpha t} \quad [1.1]$$

The urinary drug excretion rate follows Eq. [1.2]

$$\frac{dX_u}{dt} = k_e X = k_e A e^{-\alpha t} \quad [1.2]$$

The real solution of Eq. [1.2] is the cumulative urinary drug excretion-time curve, see Eq. [1.3]

$$X_u = \frac{k_e A}{\alpha} (1 - e^{-\alpha t}) \quad [1.3]$$

The total urinary excretion of the drug minus the amount excreted in urine, the residual urinary drug amount

at time t is obtained, see Eq. [1.4].

$$X_u^\infty - X_u = \frac{k_e A}{\alpha} e^{-\alpha t} \quad [1.4]$$

Eq. [1.1] is transformed to Eq. [1.5] to obtain the plasma drug concentration-time curve.

$$C = \frac{k_e A}{k_e V} e^{-\alpha t} = \frac{k_e A}{CL_r} e^{-\alpha t} \quad [1.5]$$

where CL_r can be obtained from the ratio of the urinary excretion rate to the plasma drug concentration at time t , see Eq. [1.6].

$$CL_r = \frac{\frac{dX_u}{dt}}{C_t} = \frac{k_e A}{C_t} e^{-\alpha t} \quad [1.6]$$

Scenario 2, two-compartment model after single dose *i.v.* bolus administration

The central compartment drug amount-time profile of the two-compartment distribution model after single dose *i.v.* administration follows Eq. [2.1].

$$X = Ae^{-\alpha t} + Be^{-\beta t} \quad [2.1]$$

The urinary drug excretion rate follows Eq. [2.2].

$$\frac{dX_u}{dt} = k_e X = k_e (Ae^{-\alpha t} + Be^{-\beta t}) \quad [2.2]$$

The real solution of Eq. [2.2] is the cumulative urinary drug excretion time curve, see Eq. [2.3].

$$X_u = \frac{k_e A}{\alpha} (1 - e^{-\alpha t}) + \frac{k_e B}{\beta} (1 - e^{-\beta t}) \quad [2.3]$$

The total urinary excretion of the drug minus the amount excreted in urine, the residual urinary drug amount at time t is obtained, see Eq. [2.4].

$$X_u^\infty - X_u = \frac{k_e A}{\alpha} e^{-\alpha t} + \frac{k_e B}{\beta} e^{-\beta t} \quad [2.4]$$

In general, $\alpha > \beta$, when t is sufficiently large, $\frac{k_e A}{\alpha} e^{-\alpha t} = 0$, so, in the terminal phase, Eq. [2.5] is obtained.

$$\ln(X_u^\infty - X_u) = \ln \frac{k_e B}{\beta} - \beta t \quad [2.5]$$

Eq. [2.1] is transformed to Eq. [2.6] to obtain the plasma drug concentration-time curve.

$$C = \frac{k_e A}{k_e V_c} e^{-\alpha t} + \frac{k_e B}{k_e V_c} e^{-\beta t} = \frac{k_e A}{CL_r} e^{-\alpha t} + \frac{k_e B}{CL_r} e^{-\beta t} \quad [2.6]$$

where CL_r can be obtained from the ratio of the urinary excretion rate to the plasma drug concentration at time t , see Eq. [2.7].

$$CL_r = \frac{\frac{dX_u}{dt}}{C_t} = \frac{k_e}{C_t} (Ae^{-\alpha t} + Be^{-\beta t}) \quad [2.7]$$

Scenario 3, three-compartment model after single dose i.v. bolus administration

The central compartment drug amount-time profile of the three-compartment distribution model after single dose *i.v.* administration follows Eq. [3.1].

$$X = Ae^{-\alpha t} + Be^{-\beta t} + Pe^{-\gamma t} \quad [3.1]$$

The urinary drug excretion rate follows Eq. [3.2].

$$\frac{dX_u}{dt} = k_e X = k_e (Ae^{-\alpha t} + Be^{-\beta t} + Pe^{-\gamma t}) \quad [3.2]$$

The real solution of Eq. [3.2] is the cumulative urinary drug excretion time curve, see Eq. [3.3].

$$X_u = \frac{k_e A}{\alpha} (1 - e^{-\alpha t}) + \frac{k_e B}{\beta} (1 - e^{-\beta t}) + \frac{k_e P}{\gamma} (1 - e^{-\gamma t}) \quad [3.3]$$

The total urinary excretion of the drug minus the amount excreted in urine, the residual urinary drug amount at time t is obtained, see Eq. [3.4].

$$X_u^\infty - X_u = \frac{k_e A}{\alpha} e^{-\alpha t} + \frac{k_e B}{\beta} e^{-\beta t} + \frac{k_e P}{\gamma} e^{-\gamma t} \quad [3.4]$$

In general, $\alpha > \beta > \gamma$, when t is sufficiently large, $\frac{k_e A}{\alpha} e^{-\alpha t} = 0$, $\frac{k_e B}{\beta} e^{-\beta t} = 0$, so, in the terminal phase, Eq. [3.5] is obtained.

$$\ln(X_u^\infty - X_u) = \ln \frac{k_e P}{\gamma} - \gamma t \quad [3.5]$$

The Eq. [3.1] is transformed to Eq. [3.6] to obtain the plasma drug concentration-time curve.

$$C = \frac{k_e A}{k_e V_c} e^{-\alpha t} + \frac{k_e B}{k_e V_c} e^{-\beta t} + \frac{k_e P}{k_e V_c} e^{-\gamma t} \\ = \frac{k_e A}{CL_r} e^{-\alpha t} + \frac{k_e B}{CL_r} e^{-\beta t} + \frac{k_e P}{CL_r} e^{-\gamma t} \quad [3.6]$$

where CL_r can be obtained from the ratio of the urinary excretion rate to the plasma drug concentration at time t , see Eq. [3.7].

$$CL_r = \frac{\frac{dX_u}{dt}}{C_t} = \frac{k_e}{C_t} (Ae^{-\alpha t} + Be^{-\beta t} + Pe^{-\gamma t}) \quad [3.7]$$

Scenario 4, two-compartment model after single dose p.o. administration

The central compartment drug amount-time profile of the two-compartment distribution model after single dose *p.o.* administration follows Eq. [4.1].

$$X = Ae^{-\alpha t} + Be^{-\beta t} - (A + B)e^{-k_a t} \quad [4.1]$$

The urinary drug excretion rate follows Eq. [4.2].

$$\frac{dX_u}{dt} = k_e X = k_e [Ae^{-\alpha t} + Be^{-\beta t} - (A + B)e^{-k_a t}] \quad [4.2]$$

The real solution of Eq. [4.2] is the cumulative urinary drug excretion time curve, see Eq. [4.3].

$$X_u = \frac{k_e A}{\alpha} (1 - e^{-\alpha t}) + \frac{k_e B}{\beta} (1 - e^{-\beta t}) - \frac{k_e (A + B)}{k_a} (1 - e^{-k_a t}) \quad [4.3]$$

The total urinary excretion of the drug minus the amount excreted in urine, the residual urinary drug amount at time t is obtained, see Eq. [4.4].

$$X_u^\infty - X_u = \frac{k_e A}{\alpha} e^{-\alpha t} + \frac{k_e B}{\beta} e^{-\beta t} - \frac{k_e (A + B)}{k_a} e^{-k_a t} \quad [4.4]$$

In general, $\alpha > \beta$, $k_a > \beta$, when t is sufficiently large, $\frac{k_e A}{\alpha} e^{-\alpha t} = 0$, $\frac{k_e (A + B)}{k_a} e^{-k_a t} = 0$, so, in the terminal phase, the Eq. [4.5] is obtained.

$$\ln(X_u^\infty - X_u) = \ln \frac{k_e B}{\beta} - \beta t \quad [4.5]$$

Eq. [4.1] is transformed to Eq. [4.6] to obtain the plasma drug concentration-time curve.

$$C = \frac{k_e A}{k_e V_c} e^{-\alpha t} + \frac{k_e B}{k_e V_c} e^{-\beta t} - \frac{k_e (A + B)}{k_e V_c} e^{-k_a t} \\ = \frac{k_e A}{CL_r} e^{-\alpha t} + \frac{k_e B}{CL_r} e^{-\beta t} - \frac{k_e (A + B)}{CL_r} e^{-k_a t} \quad [4.6]$$

where CL_r can be obtained from the ratio of the urinary excretion rate to the plasma drug concentration at time t , see Eq. [4.7].

$$CL_r = \frac{\frac{dX_u}{dt}}{C_t} = \frac{k_e}{C_t} [Ae^{-\alpha t} + Be^{-\beta t} - (A + B)e^{-k_a t}] \quad [4.7]$$

Scenario 5, one-compartment model after single dose i.v. infusion

The infusion time is T (h), the infusion rate is k_0 (mg/h), and the *in vivo* drug amount at the moment of T is X_T (mg). The

one-compartment plasma drug concentration–time curve for infusion administration is described in two segments, which are the infusion phase ($0 \leq t \leq T$) and the elimination phase after the infusion termination (t greater than T). The *in vivo* drug amount–time profile during the infusion phase follows Eq. [5.1].

$$X = \frac{k_0}{\alpha} (1 - e^{-\alpha t}) \quad (0 \leq t \leq T) \quad [5.1]$$

Eq. [5.1] is transformed to Eq. [5.2] to obtain the plasma drug concentration–time curve.

$$C = \frac{k_0}{\alpha V} (1 - e^{-\alpha t}) = \frac{k_0}{\alpha (X_T / C_T)} (1 - e^{-\alpha t}) \quad (0 \leq t \leq T) \quad [5.2]$$

where X_T is set approximately equal to X_0 by neglecting the elimination during infusion period.

After infusion, the elimination process is consistent with the one-compartment model after single dose *i.v.* bolus administration, see Scenario 1.

Scenario 6, one-compartment model *i.v.* infusion with multiple dosing

The infusion interval is τ (h), the function of the n th infusion phase is C_n , and the function of the n th elimination phase is C'_n , whose equations are as Eqs. [6.1,6.2].

$$C_n = \frac{k_0}{\alpha V} (e^{\alpha \tau} - 1) \frac{1 - e^{-(n-1)\alpha \tau}}{1 - e^{-\alpha \tau}} e^{-\alpha [t - (n-1)\tau]} + \frac{k_0}{\alpha V} (1 - e^{-\alpha [t - (n-1)\tau]}) \quad [6.1]$$

$$(n-1)\tau \leq t \leq (n-1)\tau + T$$

$$C'_n = \frac{k_0}{\alpha V} (1 - e^{-\alpha \tau}) \left(\frac{1 - e^{-n\alpha \tau}}{1 - e^{-\alpha \tau}} \right) e^{-\alpha [t - (n-1)\tau - T]} \quad [6.2]$$

$$(n-1)\tau + T \leq t \leq n\tau$$

Experiments

Male Sprague–Dawley rats (weight 200 ± 20 g) were randomly divided into 4 groups with 6 rats each, corresponding to the four PK scenarios without setting control groups. Group 1 was administrated with desloratadine of 0.5 mg/kg by single bolus intravenous injection. Group 2 was *p.o.* administrated with desloratadine of 2 mg/kg. Group 3 was administrated with busulfan of 2 mg/kg by single dose of 1-h intravenous infusion. Group 4 was administrated with busulfan of 1 mg/kg with a 1-h intravenous infusion for every 4 h (six times daily), for a total of 7 doses. Blood and urine samples of each single rat were collected at the specific time points or time intervals, and the plasma drug concentration and urinary

excretion amounts were determined by a validated liquid chromatography–tandem mass spectrometry (LC–MS/MS) method. Animal experiments were performed under a project license (No. IACUC–DWZX–2020–694) granted by ethics board of National Beijing Center for Drug Safety Evaluation and Research, Beijing Institute of Pharmacology and Toxicology, in compliance with National Research Council's Guide for the Care and Use of Laboratory Animals, which also in compliance with guidelines of Association for Assessment and Accreditation of Laboratory Animal Care International (AAALAC).

A clinical study was also conducted in 3 patients with leukemia, using busulfan as the test drug to validate the modeling method of Scenario 6. This study did not disturb any of the clinical treatment plan, neither increase any blood sampling for participants. Busulfan was administrated at the initial dose of 0.8 mg/kg b.w. by a 2-h *i.v.* infusion for every 6 h, for a total of 16 doses. In addition to the 6 blood sampling points in the first dose period according the original therapeutic drug monitoring (TDM) protocol, this study also scavenged 3 daily blood samples that had been collected for routine clinical testing from day 2 to 4. Other blood samples, if any, during the therapy can also be scavenged. All urine samples within 48 h of the last dosing were collected. During the sampling period, the subjects were allowed to urinate freely, while 2-h and 6-h after the end of the last infusion were set as mandatory urine sampling points. The clinical study was conducted in accordance with the Declaration of Helsinki (as revised in 2013). The study was approved by ethics board of Beijing Children's Hospital affiliated to Capital Medical University (No. [2022]–E–047–Y) and informed consent was obtained from all individual participants, or their legal guardians. The details of protocols and related concerns during either non-clinical experiments or clinical trials were listed in Appendix 1.

Modeling procedures

Figure 1 has outlined the method with Scenario 1 (one-compartment model after single dose *i.v.* bolus administration) as an example. Here, we used more complicated Scenario 2 (two-compartment model after single dose *i.v.* bolus administration) to elaborate upon the modeling procedure and related considerations.

Step 1: transformation

The cumulative amount of urinary drug excretion at time t

could be calculated by multiplying the urine concentration by the urine volume for each time interval before time t and summing up. Then, the data at each time point were transformed to the residual urinary drug amount by subtracting the cumulative excretion at each time point from the total amount of urine drug excretion (X_u^∞). This parameter was estimated by $X_u^\infty = X_u^{\text{last}} + X_u^{\text{extrap}} = X_u^{\text{last}} + V_u^{\text{last}}/\lambda$ in which λ was estimated by the linear regression of nature log of excretion rates at the last 2 time points. In essence, for this step, Eq. [2.3] was simplified to Eq. [2.4] in order to facilitate the fitting in the next step.

Step 2: fitting

The transformed urinary data were fitted according to Eq. [2.4] manually or automatically by marketed software. Although the same results could be obtained either way, the manual way was mainly introduced here to elucidate the mechanism of fitting. That is, a semi-log-linear regression was performed on the terminal phase (12, 24, and 48 h) of the residual urine drug amount according to Eq. [2.5] to obtain parameters β and $k_e B$. After substituting β and $k_e B$ into Eq. [2.5] and extending it to the alpha phase (0 to 4 h), the α -phase residuals were obtained by subtracting the amount values from the extended data of Eq. [2.5]. Then, the semi-log-linear regression was performed again on the α -phase residual data (0 to 4 h) to further obtain parameters α and $k_e A$.

Step 3: CL_r calculation

The four parameters (β , α , $k_e B$, $k_e A$) and the data on measured plasma drug concentrations at any specific time point were substituted into Eq. [2.7] to obtain the CL_r at that time point.

Step 4: anchoring

The CL_r and the obtained parameters (β , α , $k_e B$, $k_e A$) were substituted into Eq. [2.6] to determine the equation of plasma drug concentration-time curves.

Step 5: verification

In contrast to the curves fitted from urinary data, the curves directly fitted from all the measured plasma concentrations data using the corresponding compartmental models (the weight was set as equal in *WinNonlin* software) have also been calculated as an optimal fitting control. Multiple indexes were used to evaluate the fitting performance of the model, such as $\text{ratio}_{\text{AUC}}$, average folding error (AFE) and absolute average folding error (AAFE), and mean absolute percentage error (MAPE), whose definitions are listed as

follows:

$$\text{ratio}_{\text{AUC}} = \frac{\text{AUC}_{\text{pred}}}{\text{AUC}_{\text{obs}}} \quad [7]$$

The predicted value of area under the curve (AUC) was calculated by integrating Eq. [2.6] obtained from Step 4; the observed value of AUC was calculated from the measured plasma drug concentration-time data with the non-compartment analysis (NCA) using *WinNonlin* 8.0.

$$\begin{aligned} \text{AFE} &= 10 \frac{1}{n} \sum \left(\frac{\text{pred.t}}{\text{obs.t}} \right) \\ \text{AAFE} &= 10 \frac{1}{n} \sum \left| \frac{\text{pred.t}}{\text{obs.t}} \right| \\ \text{MAPE} &= \frac{1}{n} \sum \left| \frac{\text{pred.t} - \text{obs.t}}{\text{obs.t}} \right| \end{aligned} \quad [8]$$

where pred.t and obs.t represent the predicted and measured plasma drug concentrations at time t , respectively, and n represents the number of samples. If $\text{ratio}_{\text{AUC}}$ is in range of 0.5 to 2, $\text{AFE} < 2$, $\text{AAFE} < 3$, and $\text{MAPE} < 100\%$, the predicted value was considered to fit well. No further statistical test was performed.

Results

Single dose *i.v.* bolus administration

As was described in Methods, the greatest uncertainty in the modeling process arose from the selection of the compartment model in the course of fitting of urinary excretion data and the selection of the time point for the measured plasma concentration in the calculation of CL_r . Thus, to validate the effects of these two factors and to optimize the modeling process, the data on urinary excretion and plasma concentrations after a single intravenous injection of desloratadine in rats were used to evaluate the performance of the models separately constructed with the equations listed in Scenarios 1, 2 and 3, and with $\text{ratio}_{\text{AUC}}$, AFE, AAFE and MAPE as the indexes.

Figure 2 shows the plasma C-t curves retro-constructed from the urinary excretion data in an individual rat after intravenous injection of desloratadine at a single bolus dose of 0.5 mg/kg. Different compartmental models were chosen to fit the residual amount data in urine, so were different time points of the measured plasma drug concentration data to calculate CL_r . The three-compartment model (*Figure 2C*) and the two-compartment model (*Figure 2B*) were significantly better than the one-compartment model

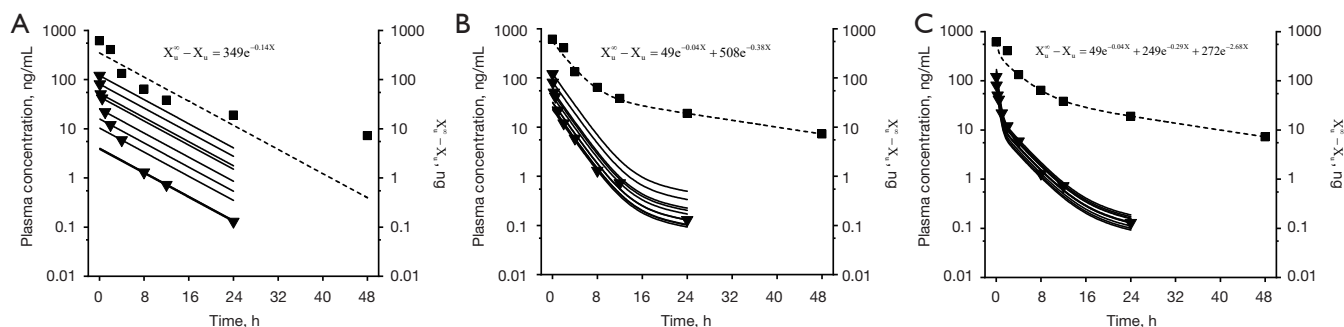


Figure 2 Retro-construction of the plasma concentration–time curves from the urinary excretion data in an individual rat after intravenous injection of desloratadine at a single bolus dose of 0.5 mg/kg. Different compartmental models [(A) one-compartment model; (B) two-compartment model; (C) three-compartment model] were chosen to fit the residual amount data in urine (■). The resulting equations are listed and the corresponding fitting curves (...) are drawn. Then, different time points of the measured plasma drug concentration data (▼) were chosen to calculate CL_r , yielding a set of different plasma concentration–time curves (—). CL_r , urinary clearance.

(Figure 2A) as judged by visual inspection. This conclusion from a single rat data was further confirmed by the statistic results of the model potency parameters, ratio_{AUC}, AFE, AAFE and MAPE, from six animals (Figure 3). As for the same compartment model, the selection of different time points of measured plasma concentrations for the calculation of CL_r resulted in different fitting errors. To be more specific, the selection of mid-term time points (1 to 8 h) of measured plasma concentrations yielded a better model than early (0 to 30 min) and late (12 to 24 h) ones (Figure 3). Ultimately, a three-compartment model with CL_r calculated from 1 h measured plasma concentration data was adopted, and the fitted curves of the six animals were plotted in Figure 4A as against the curves derived from *WinNonlin* 8.0 using the three-compartmental model fitted by all the measured plasma concentrations data. Table 1 lists the statistic results of the final model potency parameters, ratio_{AUC}, AFE, AAFE and MAPE, either for the six animals or for three patients in the respective scenario.

Single dose p.o. administration

In this part of the experiment, urinary excretion data from rats administrated with a single oral dose of desloratadine 2 mg/kg were used to construct the plasma C–t curve. After optimization as described above, it was determined that the two-compartment model was adopted and the measured plasma concentration at 4 h after administration was selected to calculate the CL_r . The resulting curves of the six animals constructed according to the equations

listed in Scenario 4 were plotted in Figure 4B as compared with the curves derived from *WinNonlin* 8.0 using the two-compartmental model fitted by all the measured plasma concentrations data.

Single dose i.v. infusion

In this part of the experiment, urinary excretion data from rats administrated with a single i.v. infusion dose of busulfan 2 mg/kg were fitted after optimization with the one-compartment model according to the equations listed in Scenario 5 and based on the selection of the measured plasma concentration at 1 hour after administration (the ending time of infusion) to calculate the CL_r . The result curves of six animals were plotted in Figure 5A as compared with the curves derived from *WinNonlin* 8.0 using the one-compartment model fitted by all the measured plasma concentrations data.

Multiple dose i.v. infusion

In this part of the experiment, urinary excretion data at the last dosing from rats administrated with 7 i.v. infusion doses of busulfan 1 mg/kg were fitted with the one-compartment model according to the equations listed in Scenario 6. Based on the optimization results derived from a single dose, it was determined that the measured plasma concentration at 1 hour after administration within the first dosing period (the end of infusion) was selected to calculate the CL_r . The result curves of the six animals were plotted in Figure 5B as compared with the curves derived from *WinNonlin* 8.0 using

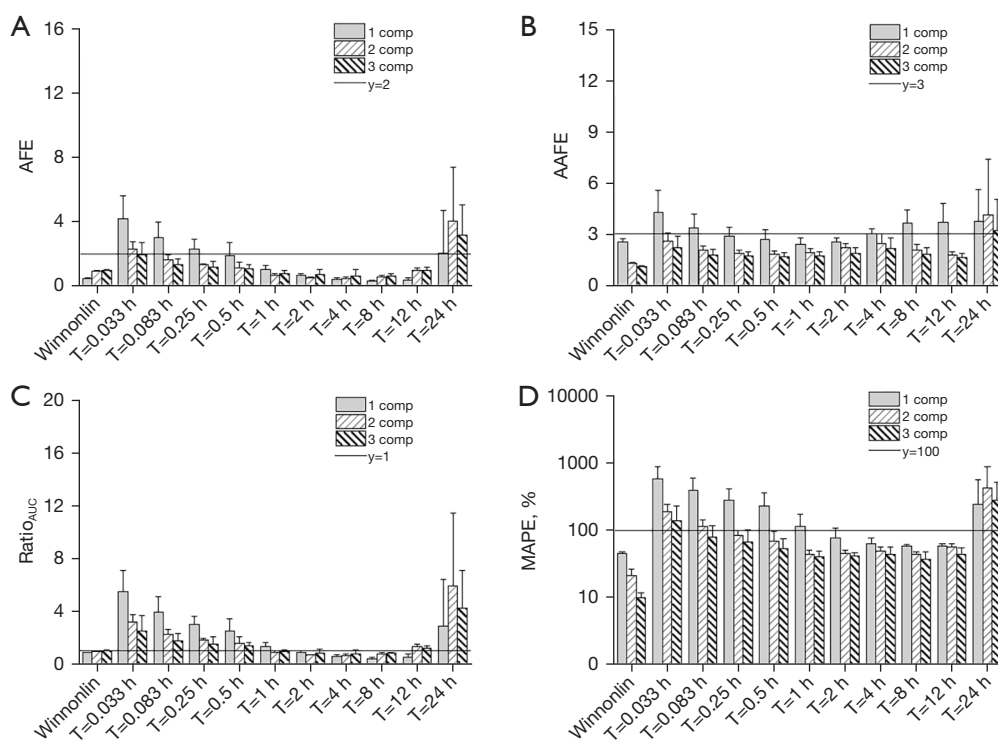


Figure 3 The modeling potency parameters of ratioAUC, MAPE, AFE and AAFE obtained by different modeling methods in rats after intravenous injection of desloratadine at a single bolus dose of 0.5 mg/kg (n=6), including those of compartmental models (Scenario 1, 2, 3) to fit the residual amount data in urine and those of time points of the measured plasma drug concentration data to calculate CL_r . Meanwhile, the parameters derived from the compartmental models fitted by all the measured plasma concentrations data using *WinNonlin* 8.0, are also listed for comparison. AFE, average folding error; AAFE, absolute average folding error; MAPE, mean absolute percentage error; AUC, area under the curve; CL_r , urinary clearance.

the one-compartment model fitted by all the measured plasma concentrations data.

This modeling scenario was also applied to clinical trials in which 3 patients were enrolled. Modeling on subjects 1 and 2 worked well except the third one with relative big errors, who suffered infection from day 2 to 4 during busulfan therapy and produced a less than normal urine sampling (*Figure 6*). It was surmised that the CL_r had changed during the urinary sampling period (last dosing) leading to a significant bias when CL_r was calculated using both urine data and the plasma concentration at 2-hour of the first dosing. The mean values of total clearance (CL) and volume of distribution of busulfan in this study were 0.21 L/h/kg and 0.69 L/kg, respectively, which are consistent with the reported pediatric median typical values (16), lower than the mean values we obtained in rats (0.27 L/h/kg and 0.95 L/kg), but higher than the reported values from adults (17).

Discussion

The data on central compartment exposure, typically presented by the plasma drug concentration-time profiles, are recognized as “critical data” of PK studies, which can shed light on the information underlying PK of drugs, such as developmental or (patho)physiological changes. The reliability and integrity of the “critical data” is critical to data quality. However, during clinical PK studies and therapeutic drug monitoring in pediatric populations, inaccessibility to the “critical data” due to ethical restrictions on blood sample collection has posed a huge obstacle to the development of pediatric medicines. Effort to explore ways to substitute urine for blood has been underway along with the development of pharmacokinetics. Basically, there are two ways to bridge between urine and plasma: one is to find the statistical relationship, and the other is to construct the mathematic equations.

The former way has been explored by Motoyasu Miura

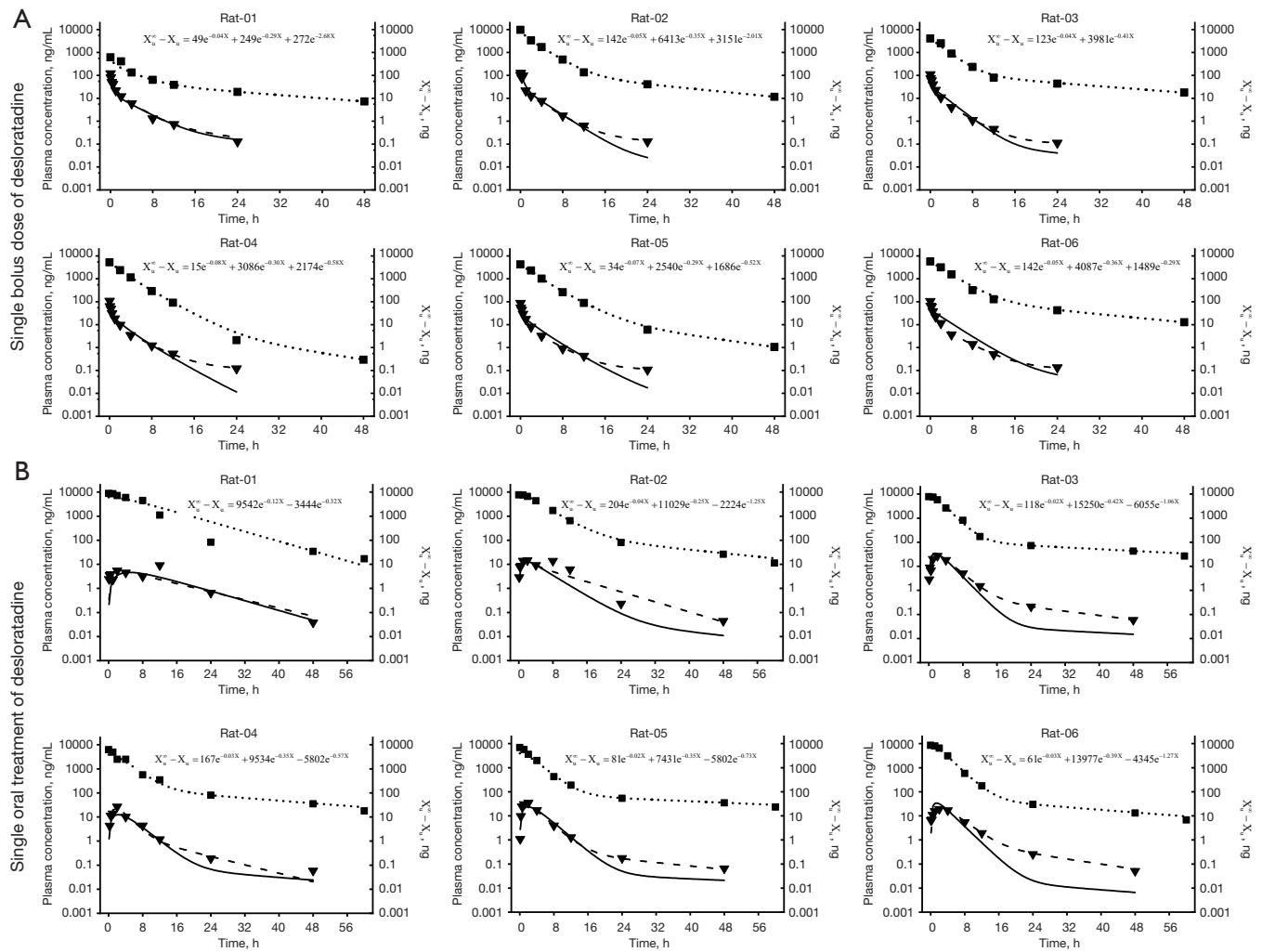


Figure 4 The plasma concentration-time curves (—) retro-constructed from the urinary excretion data by specific modeling methods in 6 individual rats after intravenous injection of desloratadine at a single bolus dose of 0.5 mg/kg (A), oral administration of desloratadine at a single dose of 2 mg/kg (B). Three- (A) or two- (B) compartment model was used to fit the residual amount data in urine (■) and the resulting equations are listed and the corresponding fitting curves (...) are drawn. The measured plasma drug concentration data (▼) at t=1 h (A), t=4 h (B), was selected to calculate CL_r . Meanwhile, the curves (---) derived from the corresponding compartment model fitted by all the measured plasma concentrations data using *WinNonlin* 8.0, are also plotted for comparison. CL_r , urinary clearance.

et al. (18), who reported the relationship between PK parameters of AUC or CL and urinary excretion or single-point plasma concentrations at various time points after patients were *i.v.* or *p.o.* administrated with midazolam (MDZ). The results showed that single-point plasma was generally superior to urinary excretion and the parent drug concentration (or excretion) was superior to metabolite/parent concentration ratio in terms of relationships and predictive accuracy. Specifically, single-point plasma concentrations at 1.5 h post-IV and 4 h post-orally

predicted AUC with the best accuracy. Nevertheless, most of the single-point plasma concentrations and urinary excretion were poorly correlated with AUC, and the metabolite/parent concentration ratio in urine was not correlated with CL. The authors of the report did not make an in-depth analysis of the reasons for these results. Our opinion was that, (I) besides the elimination process, the drug exposure in plasma was also influenced by the kinetic process of distribution. Only in one-compartment model where drug distribution rapidly reaches equilibrium

Table 1 Statistic results of the final model potency parameters in various scenarios

| Parameters | Rats (n=6) | | | | | | | | Human (n=3) | |
|----------------------|------------|------------|-------------|-------------|------------|------------|------------|------------|-------------|-------------|
| | Scenario 3 | | Scenario 4 | | Scenario 5 | | Scenario 6 | | Scenario 6 | |
| | WinNonlin | Model | WinNonlin | Model | WinNonlin | Model | WinNonlin | Model | WinNonlin | Model |
| MAPE | 10.01±1.87 | 40.22±8.32 | 32.98±15.51 | 51.31±15.98 | 16.59±8.77 | 14.73±6.52 | 12.15±7.40 | 17.25±5.20 | 21.95±7.79 | 73.90±66.81 |
| Ratio _{AUC} | 1.02±0.04 | 0.93±0.14 | 0.90±0.17 | 0.82±0.22 | 1.01±0.04 | 0.95±0.10 | 1.00±0.05 | 0.95±0.15 | 0.85±0.17 | 1.08±0.06 |
| AFE | 0.97±0.02 | 0.76±0.22 | 0.87±0.16 | 0.69±0.12 | 1.02±0.11 | 0.91±0.13 | 0.99±0.04 | 0.93±0.14 | 0.89±0.02 | 1.28±0.24 |
| AAFE | 1.11±0.03 | 1.71±0.24 | 1.38±0.35 | 1.92±0.32 | 1.14±0.05 | 1.19±0.13 | 1.13±0.08 | 1.21±0.08 | 1.09±0.12 | 1.51±0.28 |

Data are shown as mean ± standard deviation. WinNonlin: the parameters were obtained from the curves directly fitted from all the measured plasma concentrations data using the corresponding compartmental models in WinNonlin software. Model: the parameters were obtained from the plasma drug C-t curves retro-constructed from urine and single plasma data by the final model after optimization. AAFE, absolute average folding error; AUC, area under the curve; AFE, average folding error; MAPE, mean absolute percentage error; C-t, concentration-time.

in the whole body can the effect of the distribution on the plasma drug profile be neglected. However, MDZ is a typical two-compartment model (19), resulting in poor correlations between single point plasma concentrations and AUC. (II) If urinary excretion is the main contributor to drug elimination, urinary excretion of the parent drug may be positively correlated with CL. However, urinary excretion clearance of MDZ accounts for no more than 1% of the total elimination (20), and is thus subject to large individual variability in renal clearance, which is insufficient to reflect the total CL. (III) Since metabolic transformation is the main contribution of drug elimination, can the urinary metabolite/parent concentration ratio reflect the total CL? The answer is no, because metabolite exposure, besides its rate of production, is also mainly influenced by the elimination of the metabolite itself. Based on the above analysis, the predictive model based on post-hoc proportional relationships between PK parameters (AUC or CL) and single point plasma concentrations or urinary excretion is only applicable to the one-compartment model and that urinary excretion is the main elimination pathway, which is why such a model is of limited value.

Alternatively, the later way may theoretically lead to a range of widely applicable models for predicting plasma exposure curves from single-point plasma concentrations and urinary excretion, which can break down the limitations of distribution processes and urinary excretion clearance contributions. However, there is little related report so far, because there are three enormous challenges to researchers when dealing with urinary data, which are the complicated excretion mechanism, insufficient frequency sampling, and the absent volume information. Using simplified

and idealized tactics to fix these challenges, we sacrificed the precision from PBPK model with complex excretion mechanism to expediency of compartmental model in which a constant k_e is used to cover all the internal parameters. The X_u^∞ was also introduced to streamline the workflow of urine data fitting with low frequent samples. CL_r was calculated by single point plasma data, assumed that CL_r remains constant throughout the *in vivo* procedure. Despite its workability, this simplified and idealized model still has some limitations inherent to the strategies that have been identified in our validation experiments.

- (I) The multi-compartment model, three at most, limited the complexity of the fitted equations. As a consequence, take Scenario 4 Rat-01 in *Figure 4B*, this model can do nothing about the plasma exposure profile with an atypical absorption phase and mutation abnormalities, although they have already reflected in the urinary excretion curve. These problems can be partially fixed with the help of computer programming tools or PBPK software, which can facilitate the construction of plasma concentration curves in complex situations. In the meantime, increasing the frequency of urine sampling, especially in the absorption phase and the elimination phase of multi-compartment models (with multiple inflection points), may help to a more accurate curve fit.
- (II) X_u^∞ , when used to simplify the fitting equation, was dependent on the precision of the excretion rates of the last two sampling points because of its estimation method. Erratic effect of X_u^∞ uncertainty on the resulting curves can be seen in *Figure 7*,

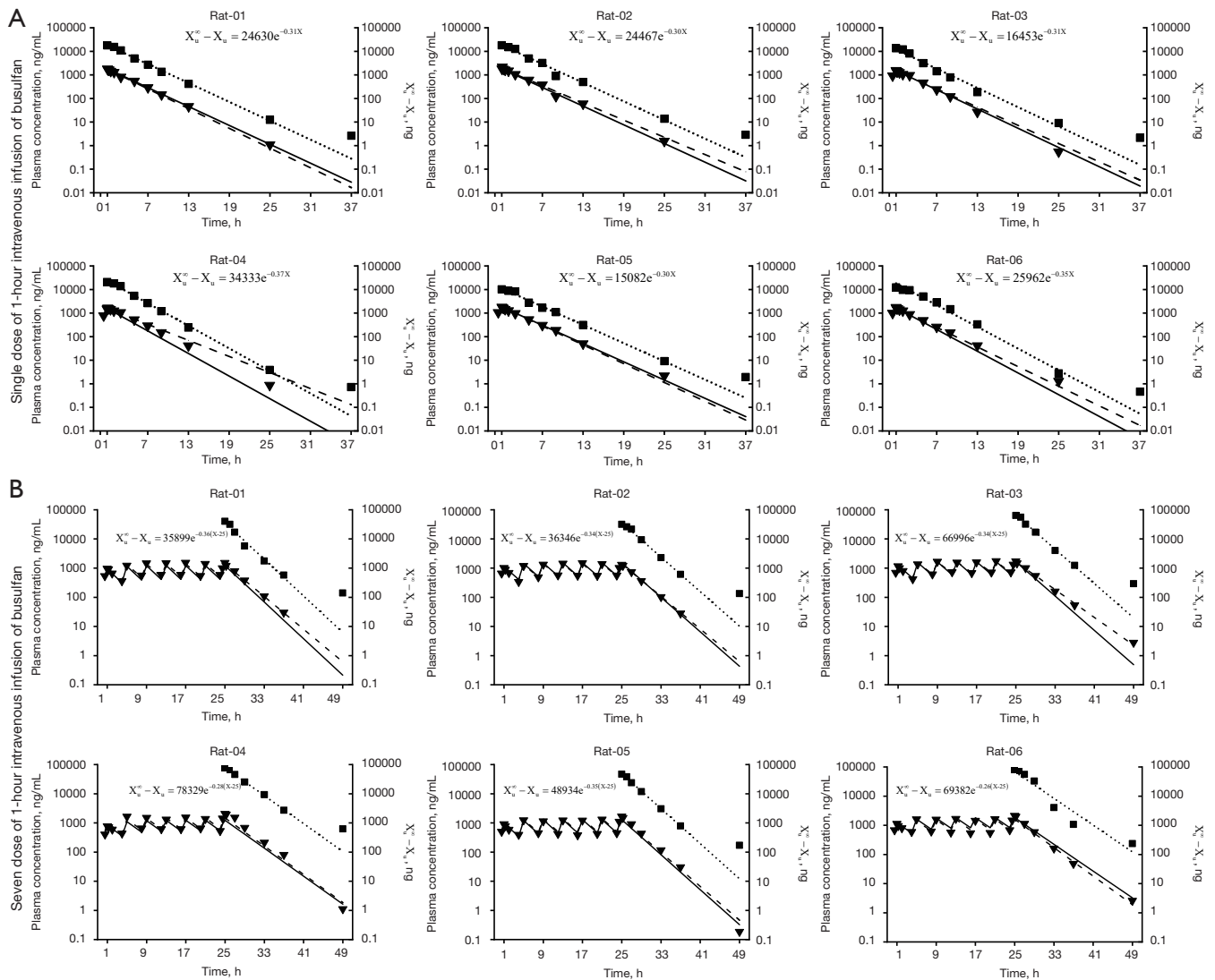


Figure 5 The plasma concentration-time curves (—) retro-constructed from the urinary excretion data by specific modeling methods in 6 individual rats after a single dose of 1-hour intravenous infusion of busulfan at 2 mg/kg (A), 7 doses of (once every 4 hours) 1-hour intravenous infusion of busulfan at 1 mg/kg (B). One-compartment model was used to fit the residual amount data in urine (■) and the resulting equations are listed and the corresponding fitting curves (···) are drawn. The measured plasma drug concentration data (▼) at $t=1$ h was selected to calculate CL_r . Meanwhile, the curves (---) derived from the corresponding compartment model fitted by all the measured plasma concentrations data using *WinNonlin* 8.0, are also plotted for comparison. CL_r , urinary clearance.

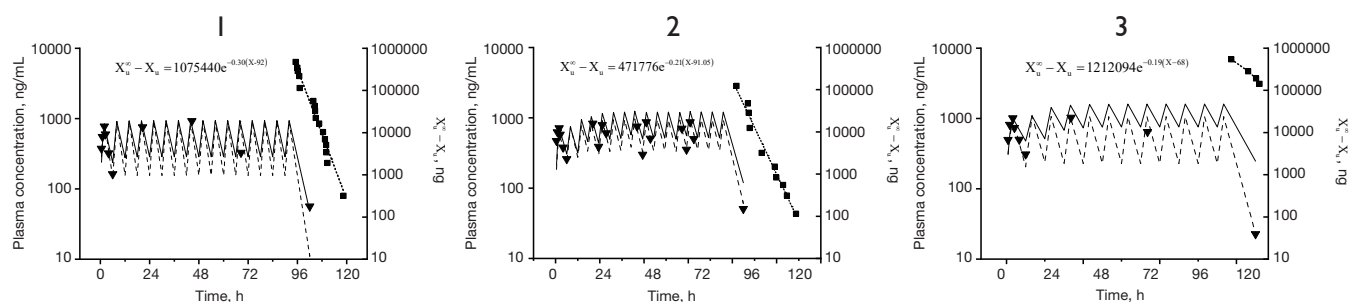


Figure 6 The plasma concentration-time curves (—) retro-constructed from the urinary excretion data by specific modeling methods in 3 individual patients after 16 doses of (once every 6 h) 1-h intravenous infusion of busulfan at 0.8 mg/kg. One-compartment model was used to fit the residual amount data in urine (■) and the resulting equations are listed and the corresponding fitting curves (···) are drawn. The measured plasma drug concentration data (▼) at t=2 h was selected to calculate CL_r . Meanwhile, the curves (---) derived from the corresponding compartment model fitted by all the measured plasma concentrations data using *WinNonlin* 8.0, are also plotted for comparison. CL_r , urinary clearance.

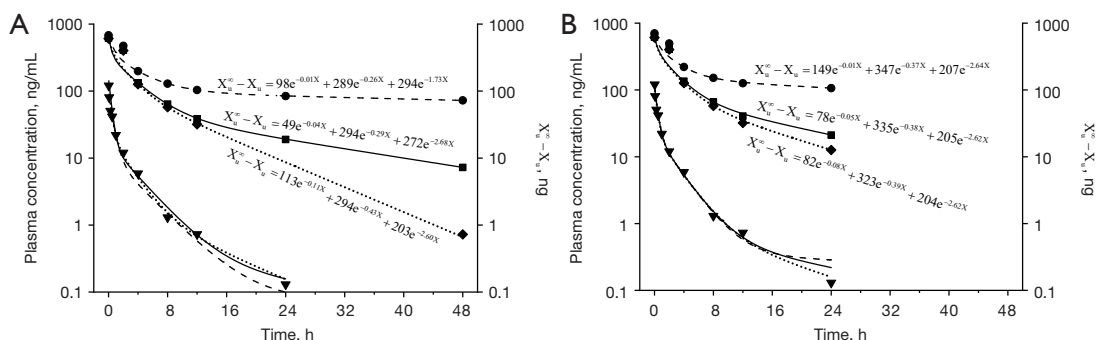


Figure 7 The influence of $X_u^∞$ estimation on the model fitting in an individual rat after intravenous injection of desloratadine at a single bolus dose of 0.5 mg/kg. The residual amount data in urine (■) was obtained by a standard modeling protocol in which $X_u^∞$ was estimated by equation 7. X_u^{extrap} was calculated to 7.26 ng (A) and 9.49 ng (B) when urine sampling up to 24 h and 48 h, respectively. The data (◆) and (●) were obtained from $0.1 \times X_u^{extrap}$ and $10 \times X_u^{extrap}$ respectively. The resulting equations of the three-compartmental model are listed and the corresponding fitting curves are drawn. In addition, the subsequent corresponding plasma concentration-time curves are plotted using t=1 h of the measured plasma drug concentration data (▼) to calculate CL_r . CL_r , urinary clearance.

which showed that inappropriate $X_u^∞$ could come to a bias plasma curve, especially in the terminal phase. Meanwhile, as compared between *Figure 7A, 7B*, a longer urine sampling time did not come to a better fitting, so clinically, urine sampling period could be sufficient in parallel with the plasma C-t curve.

- (III) A variant value of $CL_{r,t}$ was calculated from plasma drug concentrations at different time points, leading to variant bias between the predicted and observed plasma drug concentration at the non-anchored time points. Apparently, the idealization of the constant CL_r was violated. If we take $CL_{r,T} = X_u^∞ / AUC_{0-∞}$ (Eq. [8]) as the average value of the whole period,

Figure 8 shows the bias between $CL_{r,T}$ and $CL_{r,t}$ in every scenario except Scenario 6 because only partial urine was collected during multiple doses. The results showed that the most proximity of $CL_{r,t}$ to $CL_{r,T}$ was displayed in Scenario 5, while large bias and variability were exhibited in the absorption phase in Scenario 4 and elimination phase in Scenario 3. In addition, the initial phase after *i.v.* bolus administration, as shown in *Figure 8A*, exhibited a lower ratio of $CL_{r,t} / CL_{r,T}$ because of a non-linear excretion kinetic, which was not taken into account in our model. The optimal time point we selected to anchor the curve, in essence, was the

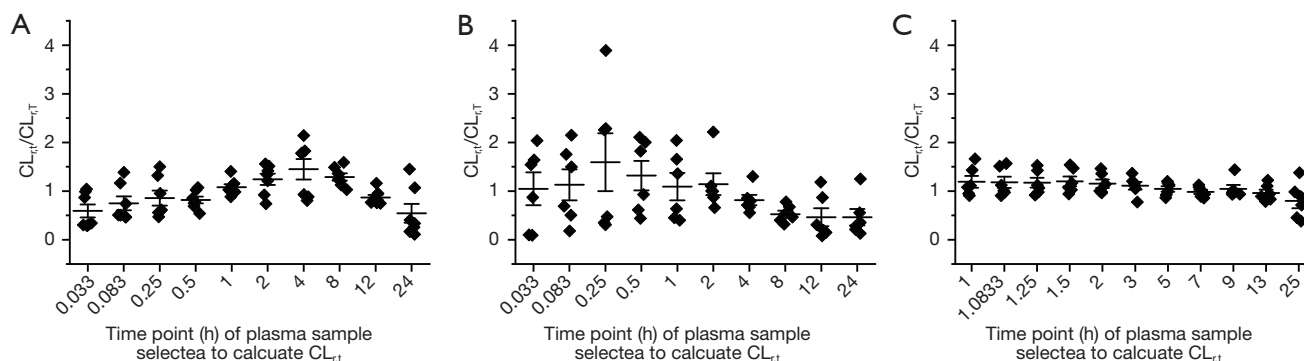


Figure 8 The ratio of $CL_{r,t}/CL_{r,T}$ in rats ($n=6$), in which $CL_{r,T}$ was calculated by Eq. [8], $CL_{r,t}$ calculated by measured plasma concentration at each time point and urine parameters obtained by different modeling scenario (A: Scenario 3; B: Scenario 4; C: Scenario 5). CL_r , urinary clearance.

time point when the $CL_{r,t}$ exhibited the minimal bias to the average $CL_{r,T}$. That might account for single-point plasma concentrations at 1.5 h post-IV MDZ with best prediction of AUC, specified by Motoyasu Miura *et al.* (18). The whole bias of the model, reflected by AFE, AAFE, and MAPE, depended on the value of $CL_{r,t}/CL_{r,T}$ at each time point. To paraphrase, the shape of plasma drug concentration-time curves could be copied to urine by a curved mirror, and the scale of its curvature determined the acceptability of our model which was simplified and idealized to a flat mirror. This drawback may be compensated for by measuring creatinine excretion or other biomarkers to evaluate renal function or by establishing a set of mechanism equations to predict temporal changes of renal clearance so that the present model could be modified to more accurate prediction. Nonetheless, regarding the modeling method presented in this paper, preliminary studies are suggested to determine the best blood sampling time point for CL_r calculation when a different drug or a different scenario is confronted clinically.

Besides the variant CL_r , another drawback of the present model was the strong dependence on a measurable parent drug in urine after administration, i.e., the *in vivo* elimination pathway of the test drug has to include renal excretion. The larger the CL_r , the more renal excretion contributes to the total elimination pathway, the larger the amount of the parent drug in urine, the smaller the variability of renal excretion clearance at each time point, and the more accurate the model will be. Although drugs with high renal excretion clearance are considered more

suitable for better performance of the model, two low urinary excretion drugs, representing the majority of market drugs, were selected in this study with aim to fulfill the clinical demands, and broader the application of this model. For drugs in the elimination pathway dominated by metabolic transformation, where the parent drug is absent or below a quantitative level in urine while metabolites are present, the plasma exposure curve of the metabolite can be constructed before being bridged to the parent drug.

Conclusions

Despite the complicated excretion mechanism, lower frequency of sampling, and poor informativeness of urine data, we employed simplification and idealization strategies in this study to develop a new method of retro-constructing plasma drug concentration-time profiles using urinary excretion and single point plasma data. Meanwhile, multiple limitations inherent to the modeling strategies were identified and 3 cases clinical data were insufficient to verify the practicability. So, more confirmative, extensive, and in-depth mechanism studies are urgently needed to make this method more robust, accurate, and generalizable for broader use. Nonetheless, the proposed method was able to deliver acceptable plasma exposure curves, shed light on the future refinements, and might promote the good practice of clinical trials in pediatric populations by updating the research paradigm, so that this vulnerable population will no longer be called “therapeutic orphans”.

Acknowledgments

Funding: This study was funded by the National Science and

Technology Major Projects for ‘Research and development of new drugs and key technologies for children’ (No. 2018ZX09721003-001-005).

Footnote

Reporting Checklist: The authors have completed the ARRIVE reporting checklist. Available at <https://tp.amegroups.com/article/view/10.21037/tp-22-505/rc>

Data Sharing Statement: Available at <https://tp.amegroups.com/article/view/10.21037/tp-22-505/dss>

Peer Review File: Available at <https://tp.amegroups.com/article/view/10.21037/tp-22-505/prf>

Conflicts of Interest: All authors have completed the ICMJE uniform disclosure form (available at <https://tp.amegroups.com/article/view/10.21037/tp-22-505/coif>). JL, HL and TZ are current employees of Guoke Excellence (Beijing) Medicine Technology Research Co., Ltd. The other authors have no conflicts of interest to declare.

Ethical Statement: The authors are accountable for all aspects of the work in ensuring that questions related to the accuracy or integrity of any part of the work are appropriately investigated and resolved. Animal experiments were performed under a project license (No. IACUC-DWZX-2020-694) granted by ethics board of National Beijing Center for Drug Safety Evaluation and Research, Beijing Institute of Pharmacology and Toxicology, in compliance with National Research Council’s Guide for the Care and Use of Laboratory Animals, which also in compliance with guidelines of Association for Assessment and Accreditation of Laboratory Animal Care International (AAALAC). The clinical study was conducted in accordance with the Declaration of Helsinki (as revised in 2013). The study was approved by ethics board of Beijing Children’s Hospital affiliated to Capital Medical University (No. [2022]-E-047-Y) and informed consent was obtained from all individual participants, or their legal guardians.

Open Access Statement: This is an Open Access article distributed in accordance with the Creative Commons Attribution-NonCommercial-NoDerivs 4.0 International License (CC BY-NC-ND 4.0), which permits the non-commercial replication and distribution of the article with the strict proviso that no changes or edits are made and the

original work is properly cited (including links to both the formal publication through the relevant DOI and the license). See: <https://creativecommons.org/licenses/by-nc-nd/4.0/>.

References

1. Wagner J, Abdel-Rahman SM. Pediatric pharmacokinetics. *Pediatr Rev* 2013;34:258-69.
2. Ince I, Solodenko J, Frechen S, et al. Predictive Pediatric Modeling and Simulation Using Ontogeny Information. *J Clin Pharmacol* 2019;59 Suppl 1:S95-S103.
3. Yu G, Zheng QS, Li GF. Similarities and differences in gastrointestinal physiology between neonates and adults: a physiologically based pharmacokinetic modeling perspective. *AAPS J* 2014;16:1162-6.
4. Ramos-Martín V, O’Connor O, Hope W. Clinical pharmacology of antifungal agents in pediatrics: children are not small adults. *Curr Opin Pharmacol* 2015;24:128-34.
5. Krekels EH, Tibboel D, Knibbe CA. Pediatric pharmacology: current efforts and future goals to improve clinical practice. *Expert Opin Drug Metab Toxicol* 2015;11:1679-82.
6. Cuzzolin L, Atzei A, Fanos V. Off-label and unlicensed prescribing for newborns and children in different settings: a review of the literature and a consideration about drug safety. *Expert Opin Drug Saf* 2006;5:703-18.
7. Hsieh EM, Hornik CP, Clark RH, et al. Medication use in the neonatal intensive care unit. *Am J Perinatol* 2014;31:811-21.
8. Shirkey H. Therapeutic orphans. *J Pediatr* 1968;72:119-20.
9. Sage DP, Kulczar C, Roth W, et al. Persistent pharmacokinetic challenges to pediatric drug development. *Front Genet* 2014;5:281.
10. Himebauch AS, Zuppa A. Methods for pharmacokinetic analysis in young children. *Expert Opin Drug Metab Toxicol* 2014;10:497-509.
11. Autmizguine J, Benjamin DK Jr, Smith PB, et al. Pharmacokinetic studies in infants using minimal-risk study designs. *Curr Clin Pharmacol* 2014;9:350-8.
12. Dumont C, Chenel M, Mentré F. Influence of covariance between random effects in design for nonlinear mixed-effect models with an illustration in pediatric pharmacokinetics. *J Biopharm Stat* 2014;24:471-92.
13. Zhou X, Dun J, Chen X, et al. Predicting the correct dose in children: Role of computational Pediatric Physiological-based pharmacokinetics modeling tools. *CPT Pharmacometrics Syst Pharmacol* 2023;12:13-26.

14. Admiraal R, van Kesteren C, Boelens JJ, et al. Towards evidence-based dosing regimens in children on the basis of population pharmacokinetic pharmacodynamic modelling. *Arch Dis Child* 2014;99:267-72.
15. Welling PG. *Pharmacokinetics Processes, Mathematics, and Applications*. Second Edition. Washington, DC: American Chemical Society, 1997.
16. Lawson R, Staatz CE, Fraser CJ, et al. Review of the Pharmacokinetics and Pharmacodynamics of Intravenous Busulfan in Paediatric Patients. *Clin Pharmacokinet* 2021;60:17-51.
17. Lin YS, Kerr SJ, Randolph T, et al. Prediction of Intravenous Busulfan Clearance by Endogenous Plasma Biomarkers Using Global Pharmacometabolomics. *Metabolomics* 2016;12:161.
18. Miura M, Uchida S, Tanaka S, et al. The Prediction of the Area under the Curve and Clearance of Midazolam from Single-Point Plasma Concentration and Urinary Excretion in Healthy Volunteers. *Biol Pharm Bull* 2019;42:1590-5.
19. Varkhede N, Patel N, Chang W, et al. A Semi-Physiologically Based Pharmacokinetic Model Describing the Altered Metabolism of Midazolam Due to Inflammation in Mice. *Pharm Res* 2018;35:162.
20. Streetman DS, Kashuba AD, Bertino JS Jr, et al. Use of midazolam urinary metabolic ratios for cytochrome P450 3A (CYP3A) phenotyping. *Pharmacogenetics* 2001;11:349-55.

Cite this article as: Li G, Zhang W, Zhang M, Xu J, Zhu G, Li J, Luo H, Zhuang X, Wang Q, Zhang T. An exploration on retro-construction of plasma drug concentration-time curves from corresponding urine excretion data and single-point plasma concentrations using a simplified and idealized method. *Transl Pediatr* 2023;12(5):845-860. doi: 10.21037/tp-22-505

Pharmacokinetic parameters of desloratadine and busulfan

The reported PK characters of desloratadine and busulfan are summarized in table S1.

Nonclinical experiments of desloratadine and busulfan

Drugs and reagents

The following drugs/reagents were used in the study: desloratadine citrate (Enrit Pharmaceutical Co., Anhui, China); busulfan for injection (Otsuka Pharmaceutical Co., Ltd, Zhejiang, China); busulfan standard (J&K Scientific Corporation, Beijing, China); verapamil (Thermo Scientific, Boston, MA, USA); propranolol (Sigma–Aldrich, St Louis, MO, USA); methanol/acetonitrile(chromatography grade; SK chemicals, Seoul, Korea); all other reagents and solvents were analytical grade.

Animals

Male Sprague-Dawley rats (weight 210 ± 20 g) were purchased from Vital River Laboratory Animal Technology Co., Ltd. (Beijing, China). The rats were fed in an exhaust ventilation cage (EVC) system, where there were free food and water, and an acclimatization period of at least 3 days preceded the experiments. Animal experiments were performed under a project license (No. IACUC-DWZX-2020-694) granted by ethics board of Beijing Center for Drug Safety Evaluation and Research, Beijing Institute of Pharmacology and Toxicology, in compliance with National Research Council's Guide for the Care and Use of Laboratory Animals, which also in compliance with guidelines of Association for Assessment and Accreditation of Laboratory Animal Care International (AAALAC).

During acclimatization, jugular vein catheterization (JVC) was carried out with silica gel tubes (Skillsmodel Biotechnology Co., Peking, China) after pentobarbital anesthesia (50mg/kg), neck shaving and routine disinfection. Following JVC, the animals were maintained on regular infusion with heparin sodium dissolved into physiological saline prior to the start of treatment. All animals were housed in exhaust ventilated closed-system cage rack (EVC) with a 12-hour light/dark cycle. The room temperature and relative humidity were maintained in the range of 22 ± 3 °C and 40–60% humidity. Experiments were performed the next day after JVC.

Dose

Twenty-four rats were randomly divided into 4 groups. Six per group were considered sufficient for evaluating model potency. Group A was administrated with desloratadine of 0.5 mg/kg for single bolus intravenous injection. Group B was administrated with desloratadine of 2 mg/kg for *p.o.* administration. Group C was administrated with busulfan of 2 mg/kg for single dose 1-h intravenous infusion and Group D was administrated with busulfan of 1 mg/kg with a 1-h intravenous infusion every 4 hours (six times daily) for a total of 7 doses. All the dosing solutions were diluted to the final concentration with physiological saline.

Collection of blood and urine samples

All the administrated rats were placed individually in metabolic cages to collect urine and feces at the prescribed time intervals. Meanwhile, about 150 μ L of blood samples was taken from the JVC canal at the set time point after administration and placed into test tubes containing heparin. The same volume of heparin sodium solution was supplemented into the rats to prevent coagulation in the canal. The obtained whole blood samples were centrifuged for 10 min (2,500 g, 4 °C) to separate the plasma before being stored at -20 °C until analysis.

To prevent the loss of urine, the rats were kept in metabolic cages throughout the experiment. Another concern was the possible residues of urinary drugs in the cages, which might cause loss on total excretion, also pollute the urine samples to be collected in the next round. Such pollution is quite likely at the beginning of experiments because of high drug excretion in urine. Thus, at least 2 sets of metabolic cages had been prepared for each animal. When urine was collected at the set time

point, the animals were directly transferred into other “clean” metabolic cages without any contamination. The used one were flushed with 70 mL methanol: water (50:50 v/v). The flushing fluid was combined with the urine sample collected at the same time interval, and the total volume was recorded before all the samples were stored at -20°C . After collection, the used cages had to be cleaned thoroughly in time for the next collection period. It was worth noting that no liquid should be lost during the operation. The urinary concentration of the drug during the terminal phase was expected to be low, so the reduced volume of the flush liquid could be used to ensure the drug concentration was high enough for determination.

Plasma samples preparation

Busulfan was extracted from rat plasma using the protein precipitation method. 50 μL of rat plasma was spiked with 50 μL methanol and 200 μL internal standard (IS) working solution (propranolol in Methanol, 20 ng/mL). To prepare calibration point samples, a stock solution was diluted with methanol to serial working solutions that ranged from 1 to 5,000 ng/mL, 50 μL of which was spiked into 50 μL of blank rat plasma and 200 μL IS working solution. The mixture was vortexed for 2 min and centrifuged at 20,000 g for 10 min before the supernatant was transferred to auto-sampler vials for LC-MS/MS analysis.

As for desloratadine, plasma samples were extracted by liquid-liquid extraction (LLE) and a 7-point standard curve (0.05, 0.25, 1.25, 6.25, 25, 125, 625 ng/mL) was prepared. 50 μL of plasma was mixed with 50 μL IS working solution (verapamil in methanol, 10 ng/mL), 50 μL of methanol or serial working solutions in methanol, vortexed, and extracted by 1 mL tert-butyl methyl ether (TBME). The samples were vortexed for 1 min, and the organic phase was collected after 10 min standing. The extraction procedures were repeated three times to improve extraction efficiency. The organic phase was merged and evaporated, and then re-dissolved with 100 μL 50% methanol (methanol: water 50:50 v/v). Samples were centrifuged at 20,000 g for 10 min at 4°C and 90 μL of the supernatant was transferred into sample vials for LC-MS/MS analysis.

Urine samples preparation

All urine samples were unfrozen on ice and vortexed for 1 min before 1 mL of urine samples was mixed with 50 μL IS solution, 50 μL of methanol or serial working solutions in methanol, vortexed, and evaporated. After being re-dissolved in 1 mL distilled water, all samples were subjected to LLE as was mentioned above.

LC-MS/MS condition

Analysis was performed on an LC-MS/MS system composed of a binary LC-30AD delivery pump, a DUG-20A5R vacuum degasser, a CTO-20A column oven, a SIL-30AC auto-sampler, a CBM-20A system controller (Shimadzu, Japan) and an LCMS-8060 mass spectrometer (Shimadzu, Japan). The mass spectrometer was equipped with an electrospray ion (ESI) source working in the positive ion multiple reaction monitoring (MRM) mode. The main MS parameters of the analyte and the respective internal standard including the transition m/z , collision energy, Q1 and Q3 voltage were listed in Table S2.

For busulfan, the mobile phase was composed of solvent A (water containing 0.1 % formic acid and 2 mM ammonium formate) and solvent B (methanol). The chromatographic separation was performed on a Kinetex C18 column (2.6 μm , 50 mm \times 3.0 mm, phenomenex, CA, USA) at a flow rate of 0.6 mL/min for 4.5 min kept at 40°C , using a gradient method of solvent B from 5% to 95% over 2.0 min, and kept for 0.5 min, and back to the initial condition over 2 min to equilibrate the column. The injection volume was set at 5 μL . The retention time was 1.63 min for busulfan and 2.06 min for IS.

For desloratadine, the mobile phase was composed of solvent A (water 0.1% formic acid with 5 mM ammonium formate) and solvent B (methanol containing 0.1% formic acid). The chromatographic separation was performed on a CAPCELLPAK C8 column (3.0 μm , 50 mm \times 2.0 mm, Shiseido, Japan) at a flow rate of 0.6 mL/min for 4.0 min kept at 40°C , using a gradient method of solvent B from 10% to 95% over 2.0 min, and kept for 0.5 min, and back to the initial condition over 1.5 min to equilibrate the column. The injection volume was set at 2 μL . The retention time was 1.67 min for desloratadine and 1.75 min for IS.

Clinical trials of Busulfan

Busulfan is a commonly used alkylating agent in the conditioning regimens of hematopoietic cell transplantation (HCT). Due to its wide pharmacokinetic (PK) variability and narrow therapeutic window, therapeutic drug monitoring (TDM) for busulfan is routinely used to individualize dosing and control the cumulative exposure.

This study was designed to assess the accuracy of PK profiles retro-constructed from urine data with comparison to results from TDM. Three patients who received intravenous busulfan conditioning regimens at Beijing Children's Hospital were enrolled from 1 March, 2022 to 31 June, 2022. The demographic data was summarized in Table S3. All patients received busulfan (Otsuka Pharmaceutical Co., Ltd., Zhejiang, China) by a 2-hour *i.v.* infusion every 6 hour and 12 or 16 doses in total. The initial dose was set as 0.8 mg/kg b.w., and subsequent doses were allowed to be adjusted by doctors according to TDM results.

The study was approved by the ethics committee of Beijing Children's Hospital (No. [2022]-E-047-Y), and written informed consent was obtained from the guardian of each patient. Based on the original TDM protocol, in which the blood sampling time point was set as 0.5, 1, 2, 2.5, 4, and 6 h after initiation of *i.v.* infusion of first dose, this study scavenged 3 daily blood samples that had been collected for clinical testing from day 2 to day 4. All urine samples within 48 h of the last administration were collected. During the sampling period, the subjects were allowed to urinate freely and all the collected urine had to be retained with accurate record of the collecting time and volume. Also, 2- and 6-h after the end of the last infusion were set as mandatory urine sampling points.

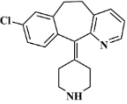
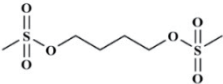
All the plasma or urine samples were stored at -20°C until analysis. The quantitative method was the same as the one used in the pre-clinical study, except that the calibrate range was changed to 1–5,000 ng/mL, and the internal standard was busulfan-d8 with MS transition 272.1→159.1, as shown in Table S4.

References

21. Zhang Y, Lu Y, Wang L, et al. Pharmacokinetics and Tissue Distribution of Loratadine, Desloratadine and Their Active Metabolites in Rat based on a Newly Developed LC-MS/MS Analytical Method. *Drug Res (Stuttg)* 2020;70:528-40.
22. Devillier P, Roche N, Faisy C. Clinical pharmacokinetics and pharmacodynamics of desloratadine, fexofenadine and levocetirizine : a comparative review. *Clin Pharmacokinet* 2008;47:217-30.
23. Zhou W, Johnson TN, Bui KH, et al. Predictive Performance of Physiologically Based Pharmacokinetic (PBPK) Modeling of Drugs Extensively Metabolized by Major Cytochrome P450s in Children. *Clin Pharmacol Ther* 2018;104:188-200.
24. Savic RM, Cowan MJ, Dvorak CC, et al. Effect of weight and maturation on busulfan clearance in infants and small children undergoing hematopoietic cell transplantation. *Biol Blood Marrow Transplant* 2013;19:1608-14.
25. Hassan M, Ehrsson H, Wallin I, et al. Pharmacokinetic and metabolic studies of busulfan in rat plasma and brain. *Eur J Drug Metab Pharmacokinet* 1988;13:301-5.
26. Hassan M, Hassan Z, Nilsson C, et al. Pharmacokinetics and distribution of liposomal busulfan in the rat: a new formulation for intravenous administration. *Cancer Chemother Pharmacol* 1998;42:471-8.
27. Molimard M, Diquet B, Benedetti MS. Comparison of pharmacokinetics and metabolism of desloratadine, fexofenadine, levocetirizine and mizolastine in humans. *Fundam Clin Pharmacol* 2004;18:399-411.
28. Wang T, Zhang K, Li T, et al. Prevalence of Desloratadine Slow-metabolizer Phenotype and Food-dependent Pharmacokinetics of Desloratadine in Healthy Chinese Volunteers. *Clin Drug Investig* 2015;35:807-13.
29. Bartelink IH, Boelens JJ, Bredius RG, et al. Body weight-dependent pharmacokinetics of busulfan in paediatric haematopoietic stem cell transplantation patients: towards individualized dosing. *Clin Pharmacokinet* 2012;51:331-45.
30. Bustami R, Khasawneh S, Absi W, et al. Bioequivalence of a fixed dose combination of desloratadine/betamethasone tablets (Oradus Beta) in healthy human volunteers. *J Bioequiv Availab* 2016;8:233-41.
31. Ghosal A, Yuan Y, Hapangama N, et al. Identification of human UDP-glucuro-nosyltransferase enzyme(s) responsible for the glucuronidation of 3-hydroxy-desloratadine. *Biopharm Drug Dispos* 2004;25:243-52.
32. Kazmi F, Yerino P, Barbara JE, et al. Further Characterization of the Metabolism of Desloratadine and Its Cytochrome

- P450 and UDP-glucuronosyltransferase Inhibition Potential: Identification of Desloratadine as a Relatively Selective UGT2B10 Inhibitor. *Drug Metab Dispos* 2015;43:1294-302.
33. Itkonen MK, Tornio A, Neuvonen M, et al. Clopidogrel and Gemfibrozil Strongly Inhibit the CYP2C8-Dependent Formation of 3-Hydroxydesloratadine and Increase Desloratadine Exposure In Humans. *Drug Metab Dispos* 2019;47:377-85.
 34. Cooper AJ, Younis IR, Niatsetskaya ZV, et al. Metabolism of the cysteine S-conjugate of busulfan involves a beta-lyase reaction. *Drug Metab Dispos* 2008;36:1546-52.
 35. El-Serafi I, Terelius Y, Abedi-Valugerdi M, Naughton S, Saghafian M, Moshfegh A, Mattsson J, Potáková Z, Hassan M. Flavin-containing monooxygenase 3 (FMO3) role in busulphan metabolic pathway. *PLoS One* 2017;12:e0187294. Erratum in: *PLoS One* 2017;12:e0190181.
 36. Ramanathan R, Reyderman L, Su AD, et al. Disposition of desloratadine in healthy volunteers. *Xenobiotica* 2007;37:770-87.
 37. Hassan M, Oberg G, Ehrsson H, et al. Pharmacokinetic and metabolic studies of high-dose busulphan in adults. *Eur J Clin Pharmacol* 1989;36:525-30.
 38. Berginc K, Sibinovska N, Žakelj S, et al. Biopharmaceutical classification of desloratadine - not all drugs are classified the easy way. *Acta Pharm* 2020;70:131-44.

Table S1 Main pharmacokinetic parameters of desloratadine and busulfan

| Parameters | Desloratadine | | Busulfan | |
|---|---|--|---|-----------------|
| | Rats | Human | Rats | Human |
| Structure |  | |  | |
| Route of administration | Oral | | <i>i.v.</i> infusion | |
| MW | 310.8 | | 246.3 | |
| Compound type | Base | | | |
| pKa | 9.7 | | | |
| Absorption (t_{max}) (h) | ~10 (21) | ~3 (22) | | |
| B/P (%) | | 2.2 (23) | | 1 (24) |
| $F_{u,p}$ (%) | | 0.16 (23) | 0.9 (25) | 0.4 (24) |
| V_{ss} (L/kg) | | 18.3 (23) | 0.67 (26) | |
| Volume of distribution V/F (L/kg) | ~52 (21) | ~49 (27) | | 0.69–0.8 (24) |
| CL/F (L/h/kg) | ~4.38 (21) | 1.5–3 (28) | 0.3 (26) | 0.22 (29) |
| Metabolites (% of dose) | | Extensive metabolism (30) | | |
| Enzymes involved in metabolism | | UGT1A1, 1A3, 2B15 (31), UGT2B10 (31), CYP2C8 (33) | GSTA1 (34) | GSTA1 (35) |
| Terminal elimination half-life (h) | ~8.5 (21) | 27 (22) | | |
| Urinary excretion (% of radioactive dose) | | 41% (22,36) | | 30% (37) |
| Urinary excretion (% of dose) | | <2% (38) | | <2% (37) |
| Faecal excretion (% of radioactive dose) | | 47% (22,36) | | |
| Faecal excretion (% of dose) | | <7% (38) | | Negligible (37) |

MW, molecular weight, in Dalton; pKa, acid-base dissociation constant; B/P, blood plasma distribution ratio; $F_{u,p}$, fraction of unbound in plasma; V_{ss} , volume of distribution at steady state; CL/F, bioavailability-corrected clearance.

Table S2 Mass spectrometric parameters for analytes in nonclinical research: precursor to fragment ion transition, voltage potential (Q1), collision energy (CE) and voltage potential (Q3)

| Analytes | MRM Transition m/z (Q1→Q3) | CE (eV) | Q1 (V) | Q3 (V) | Retention time (min) |
|---------------|----------------------------|---------|--------|--------|----------------------|
| Desloratadine | 311.30→259.05 | –21 | –16 | –28 | 1.49 |
| Verapamil | 455.30→165.10 | –29 | –19 | –15 | 1.74 |
| Busulfan | 264.10→151.10 | –11 | –14 | –16 | 1.80 |
| Propranolol | 260.10→116.00 | –19 | –14 | –13 | 2.20 |

MRM, multiple reaction monitoring.

Table S3 Demographic characteristics and body measurements of subjects

| Variable | Value |
|--------------------------------------|-----------|
| Age (years) | |
| N | 3 |
| Middium | 11 |
| Range | 10–13 |
| Gender, n | |
| Male | 2 |
| Female | 1 |
| Race, n | |
| Chinese | 3 |
| Weight (kg) | |
| Midieum | 39.5 |
| Range | 36–47 |
| Body mass index (kg/m ²) | |
| Midieum | 1.26 |
| Range | 1.23–1.40 |

Table S4 Mass spectrometric parameters for analytes in clinical research: precursor to fragment ion transition, voltage potential (Q1), collision energy (CE) and voltage potential (Q3)

| Analytes | MRM Transition m/z (Q1→Q3) | Q1 (V) | CE (eV) | Q3 (V) | Retention time (min) |
|-------------|----------------------------|--------|---------|--------|----------------------|
| Busulfan | 264.1→151.1 | -14 | -11 | -16 | 1.93 |
| Busulfan-d8 | 272.1→159.1 | -14 | -19 | -13 | 1.93 |

MRM, multiple reaction monitoring.